J Solid State Electrochem (2005) 9: 290–295
DOI 10.1007/s10008-004-0609-7

ORIGINAL PAPER

Yoshiharu Mukouyama · Mitsunobu Kikuchi
Hiroshi Okamoto

Bromide ions induced chaotic behavior in H_2O_2–H_2SO_4–Pt electrochemical system

Received: 27 August 2004 / Revised: 14 September 2004 / Accepted: 5 October 2004 / Published online: 15 December 2004

Abstract We have found a new chaotic current oscillation in the H_2O_2–H_2SO_4–Pt electrochemical system due to the addition of small amounts of bromide ions. In the system with bromide ions, an oscillation, called oscillation D, appears near the potential where another oscillation, called oscillation A, appears. The chaotic oscillation is observed in a potential region where both oscillations A and D simultaneously appear. When the electrode potential is stepped to a potential in the above region from the rest potential, a period-1 oscillation first appears for a while. A period-doubling bifurcation cascade then occurs, which is followed by a chaos. The appearance of the chaotic oscillations is explained on the basis of the reported mechanisms for oscillations A and D.

Keywords Chaos · Electrochemical oscillation · Hydrogen peroxide reduction · Platinum · Bromide ion

Introduction

Electrochemical oscillations have been reported for a variety of systems as summarized in recent reviews [1–6], including anodic metal dissolutions, cathodic metal depositions, the reductions of hydrogen peroxide, persulfate, etc., and the oxidations of hydrogen, formaldehyde, formic acid, etc. Some mathematical models based on experimental facts have recently been reported [7–12], which well explain the oscillation behavior.

The electrochemical oscillations have been classified into several categories [3–6, 13–16]. One of the most typical oscillators is the NDR oscillator, which shows a negative differential resistance (NDR) in the stationary voltammogram. This oscillator shows only current oscillations under potential controlled conditions with a sufficiently large solution or external resistance. Another typical oscillator is the HNDR oscillator, which does not show an NDR in the stationary voltammogram due to NDR-hiding factors. This oscillator shows not only current oscillations under potential controlled conditions but also potential oscillations under current controlled conditions.

Electrochemical oscillations show not only a simple periodic pattern but also chaotic or mixed-mode ones, which have been summarized in reviews [3, 4]. Those observed in the electrodissolution of metals were the most intensively studied [1, 3, 17–20]. We have been studying the potential oscillations during the oxidations of formaldehyde, formic acid, and methanol [10, 21–23], which are surface electrocatalytic reactions. The chaotic behavior observed during the galvanostatic oxidation of formaldehyde was clarified in detail [21–23]. On the other hand, current oscillations during the oxidation of formic acid have been studied by Strasser et al. [24, 25]. Their studies involved the clarification of the mix-mode oscillations.

We have also reported [15, 16, 26–29] that the H_2O_2 reduction at Pt electrodes in acidic solutions shows various types of oscillations, called oscillation A, B, C, D, and E. Oscillation A is observed in the potential region of formation of under-potential deposited hydrogen (upd-H) [26, 27], whereas oscillation B is observed in the region of hydrogen evolution [15, 26]. Oscillation E is observed when a single-crystal Pt(111) electrode is used [28]. On the other hand, oscillations C and D are observed when small amounts of halide ions are added to the solution [16, 29]. It is well known that halide ions such as chloride or bromide ion adsorb on Pt surface. The potential and time dependence of the adsorption and desorption of halide ions have been investigated in

Dedicated to Professor György Horányi to celebrate his 70th birthday in recognition of many contributions to electrochemistry.

Y. Mukouyama (✉) · M. Kikuchi · H. Okamoto
Department of natural Sciences,
College of Science and Engineering, Tokyo Denki University,
Hatoyama, Saitama, 350-0394, Japan
E-mail: mukoyama@u.dendai.ac.jp
Tel.: +81-49-296-2911
Fax: +81-49-296-2960

detail [30–37]. Based on their reports and our experimental results obtained by impedance measurements and a specular reflectance method, we could conclude that the coverage of the adsorbed halide was a slow variable for oscillations C and D [16].

Recently, we have found a chaotic oscillation observed during the reduction of H_2O_2 in the presence of bromide ions. These oscillations appeared in the potential region where both oscillations A and D were observed. This paper reports the behavior of the chaotic oscillation and bifurcation phenomena.

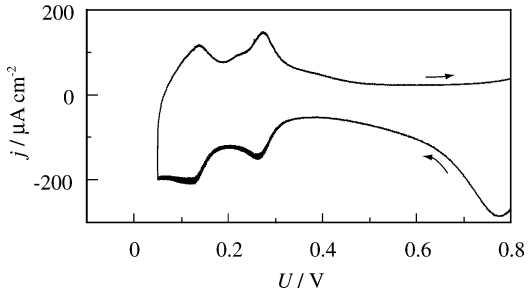

Fig. 1 A *j–E* curve under potential-controlled conditions for a Pt-disc electrode in 0.3 M H_2SO_4. The scan rate was 0.01 V s^{-1}

Experimental

The electrochemical measurements were done using a three-electrode system. A polycrystalline Pt (99.99%) disc of 1.0 mm diameter was used as the working electrode (WE). The counter electrode (CE) was a Pt-plate or a Au-plate (10×10 mm^2), and the reference electrode (RE) was a reversible hydrogen electrode (RHE). The distance between the WE and RE was 38 mm, the reason for which will be explained in the next section. The RE was placed close to the CE.

The Pt-disc electrode was prepared by cutting a Pt sphere, which was obtained by heating Pt wire in a hydrogen-oxygen flame, and sealing it with glass. It was then polished with alumina powders ranging from 3 μm to finally 0.05 μm in diameter, immersed in 60% HNO_3 for about 1 day to remove any surface contamination and then rinsed with pure water. Just before the measurements, the electrode surface was further cleaned by repeated cyclic potential scans between −0.1 and +1.85 V vs. RHE in 0.3 M H_2SO_4 (M = mol dm^{-3}) for about 60 min.

The basic electrolyte solutions were made of 0.3 M H_2SO_4–0.5 M H_2O_2. When the chaotic oscillation was studied, small amounts of KBr were added to the base solutions. The chemicals used were of special grade and water was Milli-Q water. The current density (*j*) vs. potential (*E*) and *j* vs. time (*t*) curves were measured with a potentiogalvanostat (Hokuto Denko HA-501) and an arbitrary function generator (Hokuto Denko HB-105). The measured data were recorded using an NI-DAQ card (National Instruments) at a sampling frequency of 10 kHz.

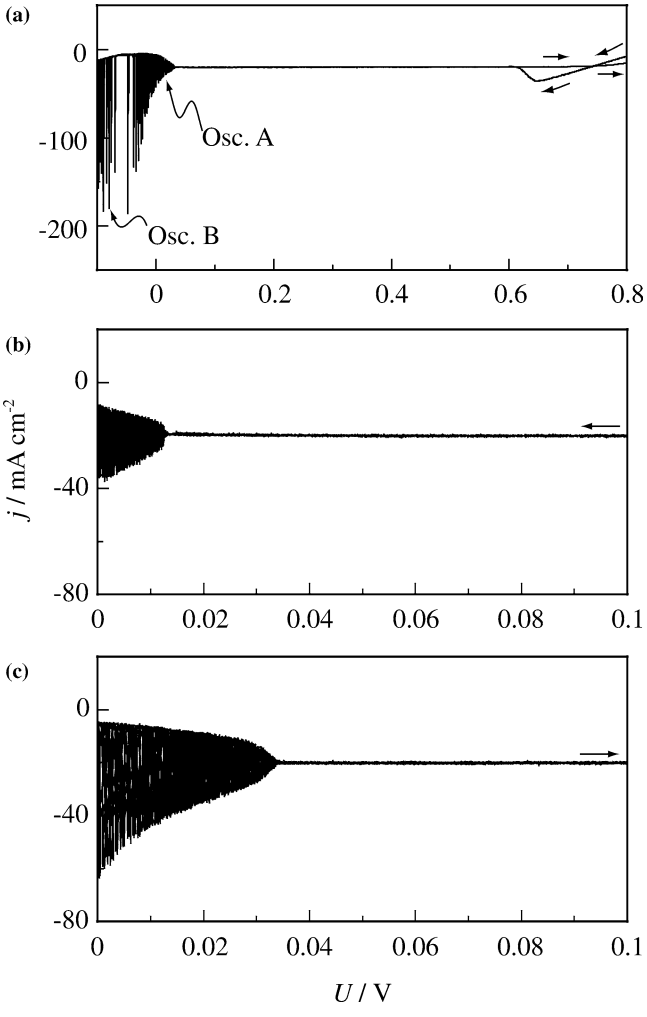

Fig. 2 A *j–E* curve under potential-controlled conditions (**a**), and enlarged curves for cathodic scan (**b**) and for anodic scan (**c**), for a Pt-disc electrode in 0.3 M H_2SO_4–0.5 M H_2O_2. The scan rate was 0.01 V s^{-1}

Results

Figure 1 shows the well-known *j–E* curve for a Pt-disc electrode in 0.3 M H_2SO_4. The scan rate was 0.01 V s^{-1}. The *j–E* curve reproduces well the essential features of polycrystalline Pt electrode. For reference in later discussions, Fig. 2 reproduces the reported *j–E* curve for a Pt-disc electrode in 0.3 M H_2SO_4–0.5 M H_2O_2. The scan rate was 0.01 V s^{-1}. The H_2O_2-reduction current started to flow at ca. +850 mV (the rest potential). Oscillation A, classified as an NDR oscillator [15, 16], appeared in the potential region where a negative differential resistance (NDR) appeared in the *j–E* curve. Oscillation B appeared in the potential region of hydrogen evolution. These were explained in Refs. [15, 16, 28, 29, 38].

The appearance of NDR has been explained as follows [27–29]: The H_2O_2 reduction is initiated by the dissociative adsorption of H_2O_2, followed by

electrochemical reduction of the resultant adsorbed OH. The NDR results from suppression of the dissociative adsorption by the formation of under-potential deposited hydrogen (upd-H). This scheme is written as follows:

$$2\,Pt + H_2O_2 \rightarrow 2Pt\text{–}OH \quad (1)$$

$$Pt - OH + H^+ + e^- \rightarrow Pt + H_2O \quad (2)$$

$$Pt + H^+ + e^- \rightleftharpoons Pt - H(upd - H) \quad (3)$$

where Pt schematically represents a surface Pt site. The coverage of upd-H is a fast species inducing the NDR, therefore we can say that at each potential a competitive adsorption equilibrium for coverage of upd-H reaches. The NDR plays an essential role in a positive feedback mechanism, as will be explained later.

Figure 3 shows *j*–*t* curves after the electrode potential (*E*) was stepped at $t = 0$ s from +850 mV (about the rest potential) to +20 mV, where oscillation A appeared for a long time (longer than 60 min) as shown in Fig. 3d. The current suddenly increased when *E* was stepped, and immediately decayed with time as shown in Fig. 3a. An aperiodic oscillation appeared in the transition state between the initial stationary current and the final stable oscillation with a period-1 pattern [38], as shown in Figs. 3b, c. The waveforms of the aperiodic oscillation became more complex as the electrode area increased and the distance between the WE and RE decreased. In this study, in order to simplify or shorten the transition state as much as possible, we used a small electrode (disc of 1.0 mm diameter) as the WE and made the distance between the WE and RE longer (38 mm) for all measurements. As a result, the aperiodic oscillation appeared for a short time (ca. 10 s). In addition, a negative global coupling [5, 6], which is likely to induce a geometrical pattern formation, was neglected, because the RE was not close to the WE.

In the previous study, we did not investigate whether or not the aperiodic oscillation in the transition state was chaotic. As shown in Fig. 3b, c, the one-dimensional Poincaré maps do not show a clear curve, which is thought to be one piece of evidence of a deterministic chaos. This, together with the absence of a period-doubling cascade, suggests that the aperiodic oscillation is not chaotic. In the map, the values of the current minimum were plotted along the horizontal axis and the values of the next minimum along the vertical axis.

Figure 4a shows a *j*–*E* curve when 300 μM KBr was added to the solution. The scan rate was 0.01 V s^{-1}. In the potential region above +500 mV, no current flowed due to high coverage of the adsorbed bromide ions. The current started to flow at ca. +500 mV and gradually increased with decreasing potential. Oscillation D, which was classified as an HNDR oscillator, began to appear at a more positive potential than oscillation A. For the cathodic scan, oscillation D appeared in the potential region below ca. +82 mV and continuously changed into oscillation A, as shown in Fig. 4b. On the other hand, in the absence of bromide ions, no oscillation was

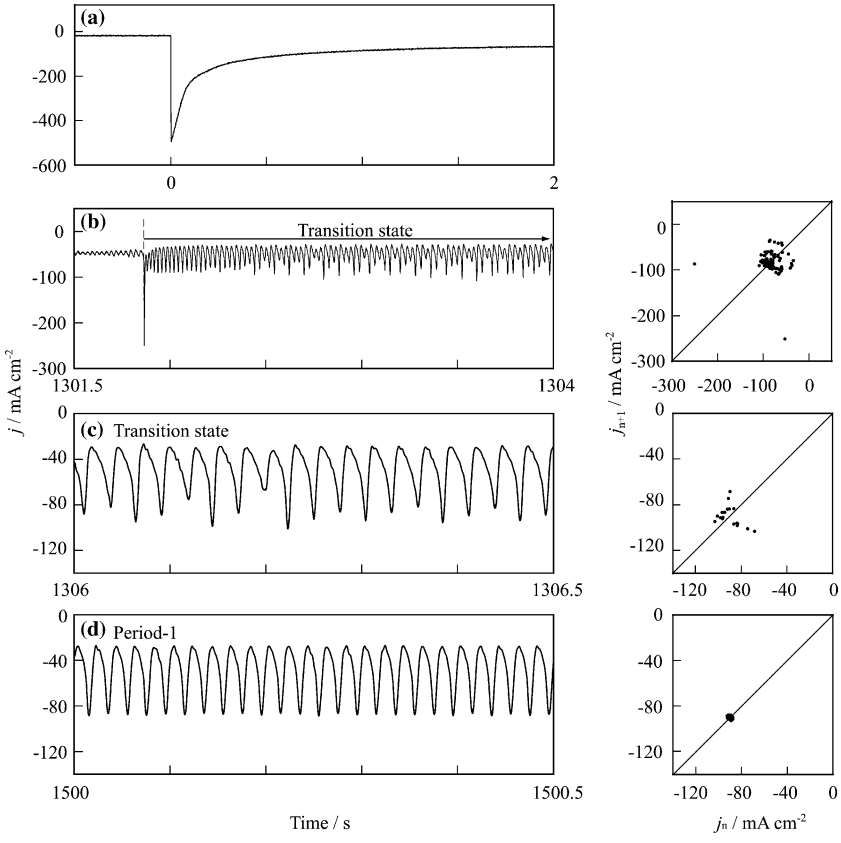

Fig. 3 *j*–*t* curves for a Pt-disc electrode when *E* was stepped from 850 to 20 mV at $t = 0$ s. The solution: 0.3 M H_2SO_4–0.5 M H_2O_2. One-dimensional Poincaré maps (return maps) are shown corresponding to the left patterns

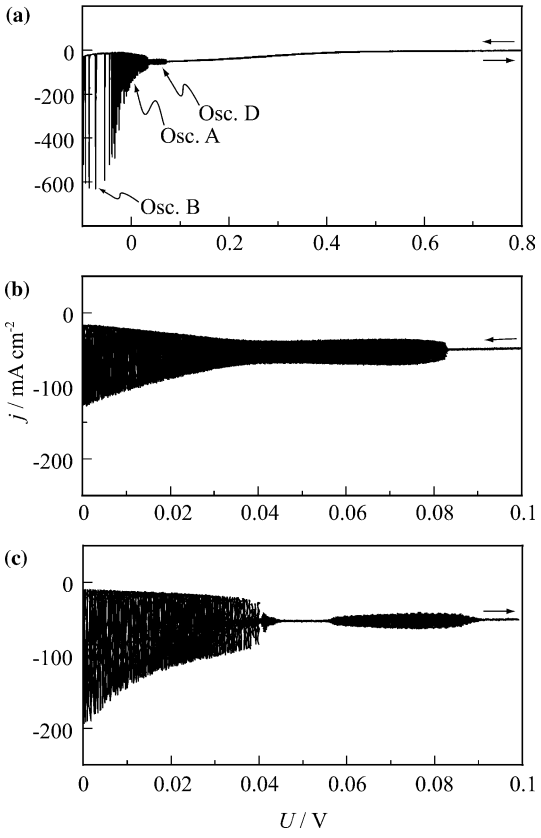

Fig. 4 A *j–E* curve under potential-controlled conditions (**a**), and enlarged curves for cathodic scan (**b**) and for anodic scan (**c**), for a Pt-disc electrode in 0.3 M H_2SO_4–0.5 M $H_2O_2$with 300 μM KBr. The scan rate was 0.01 V s^{-1}

observed in the potential region above ca. +14 mV for the cathodic scan, as shown in Fig. 2b. Therefore, it can be said that the oscillation, which appeared above ca. +14 mV and below +82 mV in the presence of bromide ions, included at least oscillation D. For the anodic scan, however, oscillation A was clearly observed in the potential region below ca. +40 mV, as shown in Fig. 4c. Accordingly, both oscillations A and D simultaneously appeared in the potential region from +40 to +14 mV. We then studied the oscillation in this potential region.

Figure 5 shows *j–t* curves in the presence of 300 μM KBr after *E* was stepped at $t = 0$ s from +850 to +20 mV. An oscillation appeared shortly after the potential step as shown in Fig. 5a. The amplitude of the oscillation observed during the first stage was greater than that of the following oscillation, probably because the surface concentration of H_2O_2 (C^s_{HO}) was high just after the potential step. A period-1 oscillation then appeared for a long time (longer than 180 s), as shown in Fig. 5a, b. A period-doubling bifurcation cascade then occurred, as shown in Fig. 5c, although the period-2^2 pattern appeared only for a short time (shorter than 0.3 s). The oscillation then became aperiodic, as shown in Fig. 5d. After this, the oscillation pattern became period-3, as shown in Fig. 5e. The oscillation period increased to around 7, one by one. The large-amplitude peak then disappeared, producing period-1 as shown in Fig. 5f, and finally the oscillation disappeared.

The aperiodic oscillation shown in Fig. 5d is probably chaotic because the period-doubling bifurcation cascade occurred before the aperiodic oscillation, as mentioned above. To verify that it was chaotic, the one-dimensional Poincaré map was plotted. The map corresponding to the aperiodic oscillation pattern showed a curve with one minimum. Figure 6 shows power spectra for the oscillations corresponding to Fig. 5c–e. The spectrum for the aperiodic oscillation shows a broader band structure, as shown in Fig. 6b, than those for the periodic oscillations such as the period-2 and period-3 oscillations. Thus, we could conclude that the aperiodic oscillation shown in Fig. 5d was chaotic.

We measured similar *j–t* curves at other potentials, and found that the complex oscillation such as period-2, 2^2, chaos and 3, etc., appeared in the potential region from +15 to +30 mV, which was included by the potential region where both oscillations A and D simultaneously appeared, +40 to +14 mV. Therefore, we think that it is necessary for the appearance of complex oscillations that both oscillations A and D appear simultaneously, as will be discussed in the next section.

Discussion

We have found a new chaotic current oscillation in the H_2O_2–H_2SO_4–Pt electrochemical system due to the addition of small amounts of bromide ions. On the other hand, the aperiodic oscillation in the transition state in the absence of bromide ions did not provide any evidence of chaos. The appearance of such an aperiodic oscillation could be explained by local (stationary) deviations in the true electrode potential, which were caused by inhomogeneous distributions of the current, and by fluctuations (local temporary deviations) in the parameters, such as *j*, the true electrode potential, C^s_{HO}, and the coverage of upd-H (θ_H) [38]. After the transition state, the oscillation pattern became stable and periodic due to the decrease in the local deviations and fluctuations. Similarly, in the presence of bromide ions, an aperiodic oscillation appeared for a short time just after the potential step, during which the oscillation was not chaotic. The appearance of the aperiodic oscillations could also be explained by the same idea as stated above. On the other hand, the chaotic oscillation occurred after the period-1 and period-doubling cascade. Therefore, the chaotic oscillations shown in Fig. 5d should essentially differ from the aperiodic oscillation observed in the transition state.

The chaotic oscillation was observed at a potential where both oscillations A and D simultaneously appeared, as mentioned in the previous section. Therefore, it is natural that the appearance of the chaotic oscillations is explained on the basis of the reported mechanisms both for oscillations A and D. Oscillation A results from two feedback loops, a fast positive and a slow negative one [26, 27]. The positive one includes an

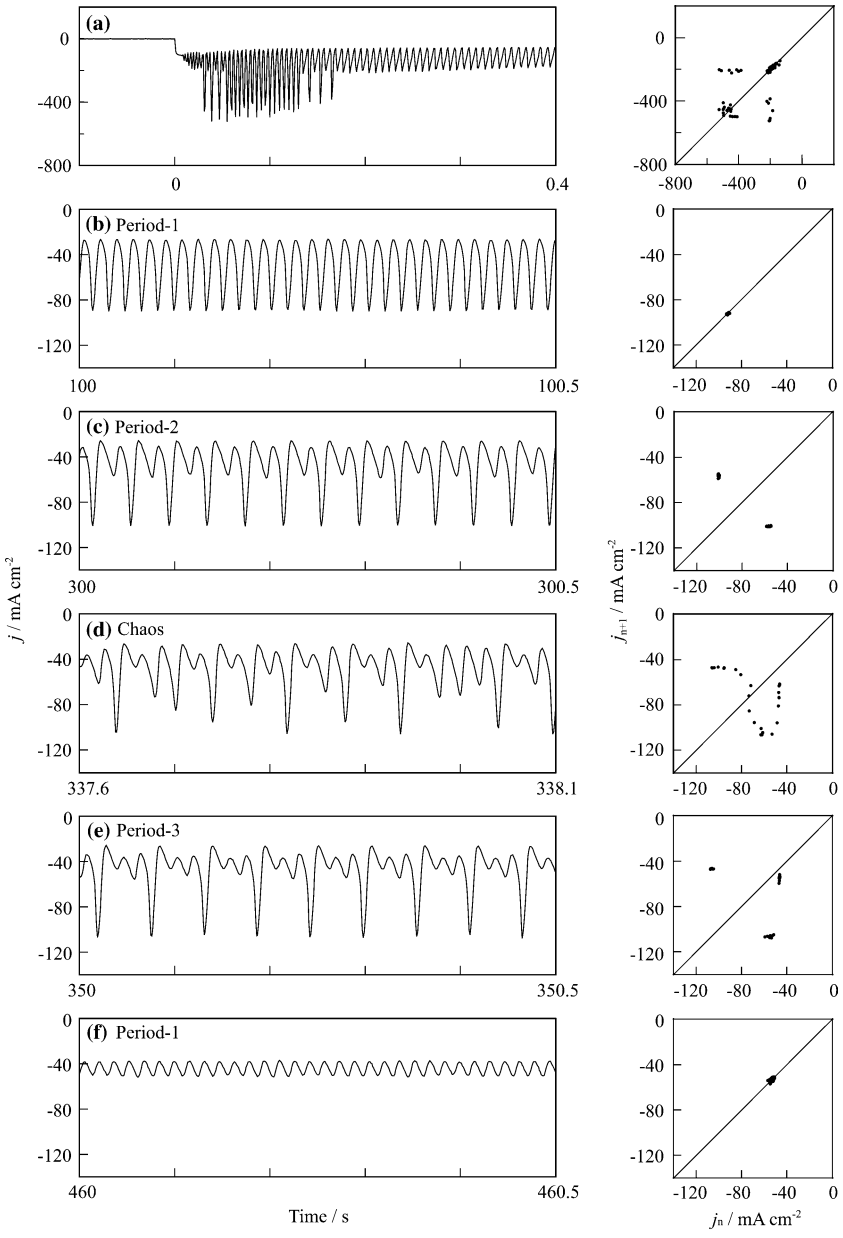

Fig. 5 *j–t* curves for a Pt-disc electrode when *E* was stepped from 850 to 20 mV at $t = 0$ s. The solution: 0.3 M H_2SO_4–0.5 M H_2O_2 with 300 μM KBr. One-dimensional Poincaré maps (return maps) are shown corresponding to the left patterns

NDR-inducing species, the adsorbed hydrogen atoms. The negative feedback loop includes C^s_{HO}. For oscillation D, we reported that there were two positive feedback loops and two negative ones [16]. One of the NDR-inducing species is the same as the species for oscillation A. One of the negative feedback loops includes the coverage of adsorbed bromide ions (θ_X). The oscillation period of oscillation D, which depends on the time scale of a slow negative feedback species, was shorter than that of oscillation A. Therefore, the simultaneous presence of two oscillations with different oscillation periods probably produces the complex oscillation patterns such as period-2, 2^2, chaos and 3, etc. In other words, we can say that the positive feedback loop and two negative feedback loops mentioned above give rise to the complex oscillation pattern, which has been pointed out by Strasser et al. [25].

In the presence of bromide ions, the period-1 oscillation observed just after the aperiodic oscillation with large amplitude, as shown in Fig. 5a, can be attributed to oscillation D, because the oscillation appears soon after the potential step in contrast to the case without bromide ions as shown in Fig. 3a, b. At +850 mV (about the rest potential) both C^s_{HO} and θ_X are high. After the potential step, the average value of C^s_{HO} and that of θ_X decrease with time. We think that the decreases in the average value of C^s_{HO} and that of θ_X tentatively cause the bifurcation. Further studies are now under way.

The H_2O_2 reduction at Pt electrodes in acidic solutions shows various types of periodic oscillations. Moreover, the system shows a chaotic one. It is quite a unique feature that such a large number of non-linear phenomena are observed in one electrode system.

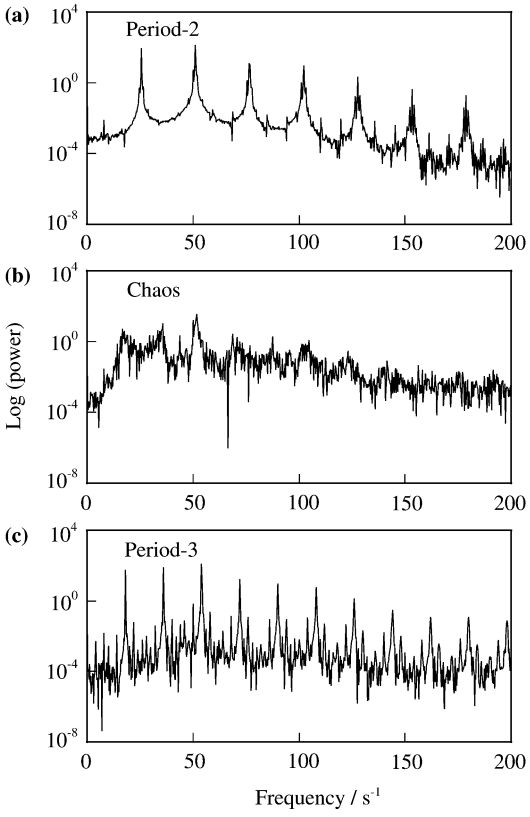

Fig. 6 Power spectra for the oscillations corresponding to the period-2 pattern shown in Fig. 5c (**a**), to chaos shown in Fig. 5d (**b**), and to the period-3 pattern shown in Fig. 5e (**c**)

Conclusion

A chaotic oscillation was observed at a potential where both oscillations A and D simultaneously appeared. When the electrode potential was stepped to this potential from the rest potential, a period-1 oscillation first appeared for a while. A period-doubling bifurcation cascade then occurred, which was followed by a chaos. After that, the oscillation pattern became period-3. The period increases to around 7, one by one. The appearance of the chaotic oscillations could be explained on the basis of the reported mechanisms for oscillations A and D.

Acknowledgments This work was partially supported by the Research Institute for Science and Technology of Tokyo Denki University Science under Grants Q03M-01 and Q04M-06.

References

1. Hudson JL, Tsotsis TT (1994) Chem Eng Sci 49:1493
2. Fahidy TZ, Gu ZH (1995) Recent advances in the study of the dynamics of electrode processes. In: White RE, Bockris JO, Conway BE (eds) Modern aspects of electrochemistry, vol 27. Plenum, New York, pp 383–409
3. Koper MTM (1996) Oscillations and complex dynamical bifurcations in electrochemical systems. In: Prigogine I, Rice SA (eds) Advances in chemical physics, vol 92. Wiley, New York, pp 161–298
4. Krischer K (1999) Principles of temporal and spatial pattern formation in electrochemical systems. In: Conway BE, Bockris JO, White RE (eds) Modern aspects of electrochemistry, vol 32. Plenum, New York, pp 1–142
5. Krischer K, Mazouz N, Grauel P (2001) Angew Chem Int Ed 40:850
6. Krischer K (2003) Nonlinear dynamics in electrochemical systems. In: Alkire RC, Kolb DM (eds) Advances in electrochemical science and engineering, vol 8. Wiley-VCH, Weinheim, pp 89–208
7. Koper MTM, Gaspard P (1992) J Chem Phys 96:7797
8. Koper MTM, Sluyters JH (1993) J Electroanal Chem 347:31
9. Wolf W, Lübke M, Koper MTM, Krischer K, Eiswirth M, Ertl G (1995) J Electroanal Chem 399:185
10. Okamoto H, Tanaka N, Naito M (1996) Chem Phys Lett 248:289
11. Strasser P, Lübke M, Eickes C, Eiswirth M (1999) J Electroanal Chem 462:19
12. Nakanishi S, Sakai S, Hatou M, Mukouyama Y, Nakato Y (2002) J Phys Chem B 106:2287
13. Koper MTM (1996) J Electroanal Chem 409:175
14. Strasser P, Eiswirth M, Koper MTM (1999) J Electroanal Chem 478:50
15. Mukouyama Y, Nakanishi S, Konishi H, Ikeshima Y, Nakato Y (2001) J Phys Chem B 105:10905
16. Mukouyama Y, Nakanishi S, Chiba T, Murakoshi K, Nakato Y (2001) J Phys Chem B 105:7246
17. Scott SK (1991) Chemical chaos. Clarendon, Oxford
18. Bassett MR, Hudson JL (1987) Chem Eng Commun 60:145
19. Bassett MR, Hudson JL (1990) J Electrochem Soc 137:1815
20. Sazou D (1997) Electrochim Acta 42:627
21. Okamoto H, Tanaka N, Naito M (1997) J Phys Chem A 101:8480
22. Okamoto H, Tanaka N, Naito M (1998) J Phys Chem A 102:7343
23. Okamoto H, Tanaka N, Naito M (1998) J Phys Chem A 102:7353
24. Strasser P, Lübke M, Raspel F, Eiswirth M, Ertl G (1997) J Phys Chem B 107:979
25. Strasser P, Eiswirth M, Ertl G (1997) J Phys Chem B 107:991
26. Matsuda T, Hommura H, Mukouyama Y, Yae S, Nakato Y (1997) J Electrochem Soc 144:1988
27. Mukouyama Y, Hommura H, Nakanishi S, Nishimura T, Konishi H, Nakato Y (1999) Bull Chem Soc Jpn 72:1247
28. Nakanishi S, Mukouyama Y, Karasumi K, Imanishi A, Furuya N, Nakato Y (2000) J Phys Chem B 104:4181
29. Mukouyama Y, Nakanishi S, Konishi H, Nakato Y (1999) J Electroanal Chem 473:156
30. Horányi G, Solt J, Nagy F (1971) J Electroanal Chem 31:95
31. Horányi G, Vértes G (1974) J Electroanal Chem 51:417
32. Horányi G, Rizmayer EM (1977) J Electroanal Chem 83:367
33. Horányi G, Inzelt G (1978) J Electroanal Chem 86:215
34. Horányi G, Inzelt G (1978) J Electroanal Chem 87:423
35. Horányi G (1980) Electrochim Acta 25:43
36. Horányi G, Rizmayer EM (1987) J Electroanal Chem 218:337
37. Bagotzky VS, Vassilyev YB, Weber J, Pirtskhalava JN (1970) J Electroanal Chem 27:31
38. Mukouyama Y, Nishimura T, Nakanishi S, Nakato Y (2000) J Phys Chem B 104:11186